PROCEEDINGS OF SPIE

SPIEDigitalLibrary.org/conference-proceedings-of-spie

Estimating standing biomass of exotic macrophytes using sUAS

Howell, Andrew, Richardson, Robert

Andrew W. Howell, Robert J. Richardson, "Estimating standing biomass of exotic macrophytes using sUAS," Proc. SPIE 11008, Autonomous Air and Ground Sensing Systems for Agricultural Optimization and Phenotyping IV, 110080Z (14 May 2019); doi: 10.1117/12.2519199

Event: SPIE Defense + Commercial Sensing, 2019, Baltimore, Maryland, United States

SPIE.

Downloaded From: https://www.spiedigitallibrary.org/conference-proceedings-of-spie on 22 Jan 2020 Terms of Use: https://www.spiedigitallibrary.org/terms-of-use

Estimating standing biomass of exotic macrophytes using sUAS

Andrew W. Howell and Robert J. Richardson
Crop and Soil Sciences, North Carolina State University,
Campus Box 7620, Raleigh, NC 27695, United States

ABSTRACT

With the advent of sUAS, research scientists and plant managers are capable of obtaining unique, fast, and low-cost quantitative data, which delivers many repeatable survey options. Benefits of autonomous sUAS platforms include minimal training, reduced human safety concerns, and creation of graphic outputs which may be readily viewed by any stakeholder who was not actively involved in the survey or management activity. Research conducted in the Wellington Region, New Zealand was used to evaluate consumer-grade sUAS technologies to map and estimate standing biomass of Manchurian Wild Rice (MWR), an exotic semi-aquatic grass which promotes flooding, and displacement of native flora and fauna. The goal of this research was to improve the speed and resolution of current survey strategies used to assess MWR among a lowland pasture site using unmanned systems and photogrammetry techniques. Image collection and data processing was conducted in a manner to provide a theoretic biomass estimation of remaining MWR following seasonal growth and herbicide applications. Post-processing methods and theories discussed attempt to identify and quantify MWR biomass using supervised imaging analysis, plant height modeling, and biomass collected *in situ*. The use of unmanned systems to map, monitor, and manage MWR is encouraged for future applications.

Keywords: sUAS, photogrammetry, invasive species, Manchurian Wild Rice, plant height modeling, biomass estimation

1.INTRODUCTION

Aquatic invasive species (AIS), such as *Zizania latifolia* (MWR; Manchurian Wild Rice), often have undesirable effects on native aquatic ecology and the associated local expenditures within invaded regions (Arnold 1959; Hofstra and Champion 2007; Santos et al. 2011; Gallardo et al. 2016). Generally, AIS like MWR reduce aquatic ecosystem biodiversity through resource competition (Madsen and Sand-Jensen 1991), dominance and displacement (Houlahan and Findlay 2004), and habitat disruption (Thum and Lennon 2009; Schultz and Dibble 2012). Specifically, the growth habits of MWR form impenetrable canopies that create waterlogged pasturelands and hazards to livestock (Figure 1). Although AIS threaten ecosystem processes (Wilcove et al. 1998), the expenditures associated with AIS are equally noteworthy as tall, perennial grass species like MWR commonly impede navigation, and obstruct canals and water intakes. To reduce the negative ecological and economic impacts associated with AIS like MWR, managers employ various schemes to protect and preserve native aquatic systems (cultural, mechanical, chemical, and monitoring tactics). One of the most effective methods to mitigate the spread of exotic plants is through early detection and rapid response measures (Westbrooks 2004) and regions which receive early detection minimize the financial and environmental costs associated with invasions (Rejmànek and Pitcairn 2002; Hestir et al. 2008; Thum and Lennon 2009; Lambert et al. 2010). However, when AIS incursions persist, such as the case with MWR in the Wellington Region, New Zealand, aquatic resource managers must integrate AIS surveillance and delimitation methods with subsequent control methods and monitoring.

It is well accepted that timely monitoring and mapping techniques are essential for evaluating native and exotic aquatic vegetation (Maceina et al. 1984; Hestir et al. 2008; Santos et al. 2011; Husson et al. 2016). Though many surveying techniques are well-established (Ackleson and Klemas 1987; Schneider et al. 2004; Gunn et al. 2010), *in situ* point-intercept sampling and 'search radius' protocols remain an industry standard for describing spatiotemporal trends in AIS presence, abundance, distribution, and richness. However, there are several hindrances with both methodologies, as assessments require a skilled workforce (correct species identification) and there is often subjectivity among surveyors, which can lower survey accuracy and efficiency. Likewise, these methods require considerable labor and time inputs, as the extent of waterway evaluations are highly correlated with the precision, spatial coverage, and time-length spent evaluating each sampling location. Therefore, researchers and plant managers seek to utilize recent advances in remote

Autonomous Air and Ground Sensing Systems for Agricultural Optimization and Phenotyping IV
edited by J. Alex Thomasson, Mac McKee, Robert J. Moorhead, Proc. of SPIE Vol. 11008,
110080Z · © 2019 SPIE · CCC code: 0277-786X/19/$18 · doi: 10.1117/12.2519199

Downloaded From: https://www.spiedigitallibrary.org/conference-proceedings-of-spie on 22 Jan 2020
Terms of Use: https://www.spiedigitallibrary.org/terms-of-use

imaging and photogrammetric technologies, specifically small unmanned vehicles (sUAS), to minimize the expenditures associated with localized AIS surveys.

For the past several decades, optical sensors (Ackleson and Klemas 1987; Sawaya et al. 2003; Nelson et al. 2006; Hestir et al. 2008) have aided in aquatic plant survey methods. Coupling remotely sensed data with computer-based programs, such as geographic information system (GIS) (eg. ArcGIS; GRASS GIS; ENVI; RStudio), has further increased the performance of mapping techniques (Lehmann and Lachavanne 1997; Shaw 2005; Santos et al. 2016, Petrasova et al. 2017). Measurements of submersed and emergent vegetation have been successfully performed using true-color and multispectral imagery (Ackleson and Klemas 1987; Peñuelas et al. 1997; Belliss and Pairman 2009; Martin et al. 2010). However, the cost of repeated applications over large spatial scales often limits the use of many of the purchased satellite flights or airborne sensors. Multispectral open-source sensors, such as Sentinel-2 and Landsat 7 TM/ETM+, do provide the basic spectral ranges needed for accessing broad population estimates, but lack the spatial and temporal resolution (e.g. pixel size of 10-30 m^2 and ~5-15 days; respectively) to represent localized vegetation or differentiate amongst similar species. Most of the compact cameras used on sUAS provide superior spatial resolution and temporal determination (e.g. pixel size of 1–3 cm^2 and minutes-to-hours), with a fraction of the economic input of a single multispectral image from a commercial airborne or satellite sensor (Baluja et al. 2012; Turner et al. 2012; Candiago et al. 2015). Nevertheless, there are limitations with true-color and multispectral platforms for acquisition of aquatic vegetation. Plant physiological and environmental factors (e.g. turbidity, sun angle geometry, weather) can create complications when evaluating some aquatic plants, especially when observing canopies partially submersed in the water column. Still, implementing a sUAS could address the above limitations, while providing superior spatial resolution (<1-5 cm^2) with a user defined temporal resolution.

The objective of this research was to serve as a pilot program to provide a timely and systematic appraisal of MWR growth, objective population dynamics, and delineate post-treatment herbicide effects of the invasive semi-aquatic plant species located in the Wellington Region, New Zealand. Specifically, this study describes capturing aerial images of MWR at varying altitudes to develop maps and estimates of plant biomass using image classifications and *in situ* collected plant metrics. A protocol for comparing *in situ* collected biomass to plant height models derived from sUAS are described to combat the aforementioned surveying limitations. Findings from this study will be useful in supporting survey options and management tools, which would remove the subjectivity of biomass estimations in the field, while providing quantitative evidence of MWR stands to stakeholders.

2.MATERIALS AND METHODS

2.1 Test Site: Wetland and low-lying pastureland (Wellington Region, North Island, New Zealand).

The study site was located near Waikanae Beach park (40°52′30″S 175°03′50″E, altitude 2-5 m AMSL), 60 km north of Wellington City (Figure 2). This invaded area has been under MWR management regimes for the past 15 years. Herbicide application via helicopter or backpack sprayers occurs annually, and occasionally twice-annually, depending on the funding year with monitoring efforts following each successive management application period. Two locations (location 1:14 ha plot and location 2: 5 ha plot; respectively) were flown at altitudes of 30, 61, and 120 m to identify the appropriate altitude needed to assess MWR stands. Destructive biomass sampling occurred among the first study location, where standing biomass was harvested from three MWR density scales using 0.25 m^2 quadrats: (N=9; 3 replications: Density 1 [0-1 m], Density 2 [1-2 m], Density 3 [>2 m]). Biomass collections represented the minimum and maximum growth structures of the invaded site. Ground control points (GCPs) were distributed randomly across both study locations (Table 1; Figure 3). The GCPs were represented using latex party balloons inflated to a diameter of 18 cm and attached to emergent vegetation or fencing using monofilament fishing line (Figures 3,4). Each GCP position was measured using a handheld global positioning system (GPS, Garmin Rino 650, Australia/New Zealand) with 3 m horizontal and vertical position accuracy.

2.2 Biomass sampling.

Downloaded From: https://www.spiedigitallibrary.org/conference-proceedings-of-spie on 22 Jan 2020
Terms of Use: https://www.spiedigitallibrary.org/terms-of-use

Destructive aboveground biomass sampling ensued separately amongst the sampling sites within the first study area (Table 2). Aboveground tissue (above soil or waterline) samples were cleaned of other plant materials and detritus. Harvested leaves representing each density level were bundled using bailers twin and measured for average leaf length prior to drying. To obtain above-ground dry biomass, each of the samples were dried to a constant dry-mass at 30 °C for 2 weeks, and each plant bundle weighed separately.

2.3 sUAS platform.

In this study, a DJI Phantom 4 Advanced quadcopter was used to capture aerial photography of the study sites. The flight duration varied between 3–24 minutes based upon the altitude and flight plan. Due to battery and environmental conditions, flights were conducted over two days between the hours of 10:00 and 14:00 (18 April and 19 April). Pix4D Mapper and DroneDeploy tablet applications were used to develop and conduct each flight plan. Contingent on the flight application used, the DJI provided gimbal mounted RGB optical sensor (20 MP; FOV 84° 8.8 mm) maintained near-nadir and slightly oblique camera positions throughout the duration of each fight mission. During each flight, environmental conditions and sUAS locations were manually monitored and recorded. Captured imagery and associated metadata was automatically logged to an onboard 32 GB SD memory card.

2.4 Image pre- and post-processing.

To produce an orthomosaic image and digital surface model (DSM) from each flight plan, Agisoft PhotoScan Pro photogrammetric structure from motion (SfM) software was utilized. The first process in creating a projected DSM and orthomosaic was to align the photos then assign GCPs to the imagery workspace. To successfully reference each GCP, at least three images containing each unique GCP was required. To help optimize the alignment process, GCPs were filtered by photo markers to use GCP .txt file coordinates for spatial error reduction. Prior to building dense clouds, the boundary box containing each region of interest was resized to encompass only the minimal extent of the model elements to reduce processing time and increase efficiency. For point cloud (Figure 5), mesh, and texture construction, a medium resolution batch process was used. Parameters for DSM and orthophoto creation were obtained from batch processing results. Data exports (.tiff) for further processing and reports (.pdf) were exported for further spatial error analysis.

Additional GIS processing occurred using ESRI's ArcGIS 10.4.1, QGIS 2.18, and GRASS GIS 7.4.0. Only orthophotos and DSMs from the first study location at 61 m were used to develop model parameters for supervised image analysis, plant heights, and point cloud differences among LiDAR (1 m) digital elevation model (DEM) and SfM results (Figure 6). The DSMs were resampled to represent the biomass sampling quadrat area (0.25 m^2). Biomass collection points were associated among each orthophoto to confirm well-known MWR stands for image classification training sample selection. Identified MWR stands from the classification techniques were then extracted from the resampled DSM to provide a raster dataset representative of MWR plant height estimates derived from the sUAS (Figure 7).

2.5 Statistical analysis and modeling.

Regression analysis and biomass prediction algorithms utilized RStudio base, nonparametric, and ggplot2 packages (Hayfield and Racine 2008; Wickham 2009; R Core Team 2018). Employing ArcGIS 10.4.1 raster calculator, plant height raster datasets were imported into the MWR biomass regression, developed from *in situ* collected plant height estimates and biomass bundles, to acquire dry biomass estimates of the othrophoto scene.

3.RESULTS AND DISCUSSION

Due to the complexity of plant community diversity among the test sites, and thus the requirement to classify individual MWR plant stands, only the 61 m flight altitude results for this study are presented to provide a proof-of-concept.

Imaging parameters: *image capture:* 61 AGL; *fight time:* 10 minutes; *area coverage:* 13.61 ha; *camera N* = 157 images.

3.1 Study site characteristics.

Downloaded From: https://www.spiedigitallibrary.org/conference-proceedings-of-spie on 22 Jan 2020
Terms of Use: https://www.spiedigitallibrary.org/terms-of-use

While MWR was the only species of interest in this study, two other similarly structured species were present in the image scenes, which included *raupō* (Cattail; *Typha* spp.) and *harakeke* (New Zealand flax; *Phormium tenax*). Each alike species (in terms of aerial discrimination) was heterogeneously distributed among the imaged portions of the landscape. This plant distribution pattern did not impede image correlation with MWR, as biomass samples collected *in situ* were selected among sites comprising < 5% non-MWR species so not to skew the biomass prediction equation during analyses.

3.2 Plant height and biomass estimations.

Although our plant presence classification methods likely overestimated the presence of MWR, note that identified MWR regions were co-referenced with flight logs procured during the previous year's helicopter application treatment. This allowed for a direct correlation between computer based image classifications of MWR and known MWR populations among the target sites identified by the aerial applicators.

Quadrat collection sites throughout the defined experimental area represented a wide range of plant heights, biomass, and MWR stand densities to account for growth variability (density height means = 143-276 cm; density weight means = 210-1812 g dm). Biomass collections varied less among Density level 1, than Density levels 2 or 3. Mean plant height to dry-mass ratios notably differed among each sampling density (Density 1: 2.26; Density 2: 6.96; Density 3: 5.34), suggesting that plant height per unit area is an important factor to consider when describing expanses of low growth plant stands.

Comparing the *in situ* acquired plant heights and biomass provided a regression equation used for importing the MWR classified sUAS imagery (Figure 8). Biomass estimates showed strong agreement with MWR plant height and density estimates collected in-field ($r^2_{adj} = 0.61$). While variation among plant density levels are presented, our trends suggest a pattern of linearity, with the greatest deviance produced among plant stands 1.5-2.5 m tall. Employing the *in situ* trained regression equation with raster algebra and classification statistics, we estimate the MWR plant stands represented in location 1 (13.61 ha) at 985.79 kg dry mass (Figure 9). Though we recognize this estimate is likely location specific, and possibly altitude dependent if image classification is required, future-imaging missions over this location may desire to use or estimate as a baseline measurement to compare future estimates.

3.3 Survey methods and equipment.

The Phantom 4 Advanced sUAS operated completely autonomously using a mission developed through PiX4D Mapper mobile application, which allowed for image capture repeatability and transfer of missions over time. Not only does this procedure reduce spatial coverage errors for future comparisons, but allows those unfamiliar with the equipment or study site to collect data without recreating the original flight plan. We also found no issue with camera image alignment amongst any of the imaging missions above 30 m (only 1 image went unaligned at the lowest altitude tested) during processing using this methodology.

We found using GCPs was critical when developing plant height estimates and fixing relative location errors. While the GCPs used in this study provided a quick solution for not having fixed GCPs in the landscape, we suggest future applications among semi-aquatic environments use static georeferenced GCPs if forthcoming flights are scheduled (eg. 6-8 GCPs per imaged site, with each GCP represented by a permanent pole with a distinguishable terminal target). One issue, which can arise using balloon GCPs, is if wind gusts are present the chance of the balloons deflating increases. Furthermore, while relative accuracy is increased using inflatable GCPs, the spatial precision can decrease due to windy conditions. We also make awareness that a precision GPS with fine resolution (5-10 cm vertical accuracy) should be implemented when placing GCPs. Nevertheless, our results show that relative accuracies can achieve biomass estimations of exotic macrophytes.

3.4 Future biomass estimation research.

Among future studies, metrics of interest might include how patchy distributions of MWR in an orthomosaic scene accounts for biomass prediction success. For example, how does biomass calculation under scenarios of high plant diversity compare with monoculture stands? Likewise, what effect does plant morphology and phenology have on

Downloaded From: https://www.spiedigitallibrary.org/conference-proceedings-of-spie on 22 Jan 2020
Terms of Use: https://www.spiedigitallibrary.org/terms-of-use

detection ability among sites with similarly structured species? Based on our findings, there remains a further need to determine how plant stand densities (number of plants per unit area and true spatial surface area) affects aerially derived biomass estimations.

Some example equipment and methods requiring further testing to overcome some of the known limitations include:

- *Survey grade GPS equipment*
- *Fixed Ground Control Points*
- *sUAS with RTK/PPK capabilities*

4.CONCLUSION

Mapping is crucial for risk assessment of plant invaders, quantifying ecosystem changes, and providing sound tactics for water resource conservation, management, and stewardship. This study defines additional toolsets and protocols, using photogrammetric and GIS strategies, to meet mapping demands. With the rapid development of off-the-shelf sUAS platforms, the potential exists to incorporate unmanned technologies into monitoring and mapping strategies for MWR control efforts. These tools may additionally be incorporated with traditional methods, such as 'search and locate' surveys, so that managers have the benefits of each technique. Implementing autonomous sUAS could provide an additional cost-effective and consumer available toolset which is scalable and provides a reproducible method for MWR monitoring and management. Based on results, we suggest that our sUAS equipment and image capture strategies defined in this study are capable of providing greater than proof-of-concept evidence for MWR aerial biomass estimation. Not only does an aerial biomass assessment provide greater objectivity by the surveyor than manual binary estimates (eg. presence/absence from ground or helicopter GPS tagging) but also allows for repeatable survey applications. This low-cost system is capable of providing parallel among many emergent aquatic species, systems, and environments. Likewise, this innovative research will prove useful in the invasive plant management industry as remote image collection and photogrammetric advancements progress. The data and information collected from sUAS surveys will contribute to the successful management, sustainability, and stewardship of agricultural and environmental resource systems in the future (Adam et al. 2010; Baluja et al. 2012; Vega et al. 2015). Estimating standing biomass of an exotic macrophyte species like MWR is crucial in monitoring successional growth and eradication program efforts. Findings from this study may be used for stakeholder reporting and management prescriptions.

5.MANAGEMENT IMPLICATIONS

Annually, the New Zealand biosecurity force and third-party researchers, conduct widespread surveillance to determine new infestations and prevalence of MWR plant stands. Traditional methods of this operation include manned helicopters and wading surveys using legacy or predicted infestation areas. This system requires a well-skilled workforce of many experienced professionals with extensive knowledge in piloting safety, significant familiarity with localized plant population dynamics, equipment upkeep, and is often difficult to repeat consistently on a multi-year program. The cost efficiency of this current regime could be increased if there were reductions to labor, time, and safety concern confronted with these surveys. Unmanned aerial technologies require minimal training, remove most human safety concerns, and provide deliverables, which may be viewed by any stakeholder within minutes to hours.

Estimates of MWR coverage, distribution, and biomass have been collected over the last decade in many areas within the North Island, NZ regions. These estimates have traditional been used to assess the vigor and impact MWR has had on a particular region for the fiscal or calendar year. Annually, active management has occurred following these plant survey assessments, which has included physical plant removal alongside herbicide treatment programs. Monitoring and assessing the temporal success or trends that follow these management regimes has become a costly and time intensive investment.

Downloaded From: https://www.spiedigitallibrary.org/conference-proceedings-of-spie on 22 Jan 2020
Terms of Use: https://www.spiedigitallibrary.org/terms-of-use

Outcomes from this study may also be suited to correlate legacy-data biomass estimates held by stakeholders. Imagery may be further subjected to a variety of other post-processing models to identify and quantify pre- and post-herbicide treatment effects using machine-learning, image classification (eg. Canopeo mobile application), and geostatistical techniques. Waterway documentation and image capture intervals of vegetative growth could occur prior, during, and at set intervals after herbicide treatment (e.g. 2, 4, and 8 WAT) to provide a timeline of spectral or growth form response of MWR. For example, temporal and spatial persistence of MWR after treatment could follow visual ratings of percent control (efficacy appraisals of chlorosis and necrosis) from 0% (no injury) to 100% (complete desiccation) and automated imaging appraisals. Parallel treatment assessments of helicopter locations (monitored with GPS) versus backpack applications may follow an identical imagery protocol for comparison.

ACKNOWLEDGEMENTS

We would like to acknowledge the contributions of our collaborators and supporters with the aquatic plants group at National Institute of Water and Atmospheric Research, the Pest Plants Division at Greater Wellington Regional Council, and Kieran McLean for assistance with data collection.

REFERENCES

[1] Arnold, E.H. 1959. Manchurian rice grass. Proceedings of the NZ Weed Control Conference 12: 82–84.
[2] Hofstra, D. and Champion, P. 2007, 28:2. Stopping the freshwater wild rice invader. Retrieved from: https://www.niwa.co.nz/aquatic-biodiversity-and-biosecurity/update/issue-05-2003/stopping-the-freshwater-wild-rice-invader.
[3] Santos, J.S., Anderson, L.W., and Ustin, S.L. 2011. Effects of invasive species on plant communities: an example of using submersed aquatic plants at the regional scale. Biol. Invasions. 13:443-457.
[4] Gallardo, B., Clavero, M., Sánchez, M.I., et al. 2016. Global ecological impacts of invasive species in aquatic ecosystems. Global Change Biology. 22(1):151-163.
[5] Madsen, T.V., Sand-Jensen, K. 1991. Photosynthetic carbon assimilation in aquatic macrophytes. Aquat Bot 41:5–40.
[6] Houlahan, J. and Findlay, C. 2004. Effect of invasive plant species on temperate wetland plant diversity. Conservation Biology. 18(4):1132-1138.
[7] Thum, R. and Lennon, J. 2009. Comparative ecological niche models predict the invasive spread of variable-leaf milfoil (Myriophyllum heterophyllum) and its potential impact on closely related native species. Biological Invasions. 12(1):133-143.
[8] Schultz, R. and Dibble, E. 2012. Effects of invasive macrophytes on freshwater fish and macroinvertebrate communities: The role of invasive plant traits. Hydrobiologia. 684(1):1-14.
[9] Wilcove, D.S., Rothstein, D., Dubow, J., et al. 1998. Quantifying threats to imperiled species in the United States. BioScience. 48(8):607-615
[10] Westbrooks R. 2004. New approaches for early detection and rapid response to invasive plants in the United States. Weed Technology. 18:1468-1471.
[11] Rejmànek, M. and Pitcairn, M.J. 2002. When is eradication of exotic pest plants a realistic goal? In C. R. Veitch and M. N. Clout, eds. Turning the Tide: The Eradication of Invasive Species. Gland, Switzerland: IUCN SSAC Invasive Species Specialist Group. 249–253.
[12] Hestir, Erin.L., Khanna, S., Andrew, M.E., et al. 2008. Identification of invasive vegetation using hyperspectral remote sensing in the California Delta ecosystem. Remote Sensing of Environment. 112(11):4034-4047.
[13] Lambert, A.M., Dudley, T.L., Saltonstall, K. 2010. Ecology and impacts of the large-statured invasive grasses Arundo donax and Phragmites australis in North America. Invasive Plant Science and Management. 3:489-494.
[14] Maceina, M.J. and Shireman, J.V. 1980. The use of a recording fathometer for determination of distribution and biomass of hydrilla. J. Aquat. Plant Manage. 18:34-39.
[15] Husson, E., Ecke, F., and Reese, H. 2016. Comparison of Manual Mapping and Automated Object-Based Image Analysis of Non-Submerged Aquatic Vegetation from Very- High-Resolution UAS Images. Remote Sens 8(9):724.

Downloaded From: https://www.spiedigitallibrary.org/conference-proceedings-of-spie on 22 Jan 2020
Terms of Use: https://www.spiedigitallibrary.org/terms-of-use

[16] Ackleson, S.G. and Klemas, V. 1987. Remote Sensing of Submerged Aquatic Vegetation in Lower Chesapeake Bay: A Comparison of Landsat MSS to TM Imagery. Remote Sens Environ 22:235–248.
[17] Schneider, P., Burczynski, J., and Sabol, B. 2004. Case studies for the evaluation of Submersed Aquatic Vegetation (SAV) using hydroacoustics as a dedicated assessment tool. ICES 2004 Annual Science Conference, 22–25 September, Vigo, Spain.
[18] Gunn, I.D.M., O'Hare, M., Carvalho, L., et al. 2010. Assessing the condition of lake habitats: a test of methods for surveying aquatic macrophyte communities. Hydrobiologia 656(1):87–97.
[19] Sawaya, K.E., Olmanson, L.G., Heinert, N.J., et al. 2003. Extending satellite remote sensing to local scales: Land and water resource monitoring using high-resolution imagery. 88:144-156.
[20] Nelson, S.A.C., Cheruvelil, K.S., and Soranno, P.A. 2006. Satellite remote sensing of freshwater macrophytes and the influence of water clarity. Aquat Bot 85:289–298.
[21] Lehmann, A. and Lachavanne, J.B. 1997. Geographic information systems and remote sensing in aquatic botany. Aquat Bot 58:195–207.
[22] Shaw, D.R. 2005. Translation of remote sensing data into weed management decisions. Weed Sci. 53(2):264–273.
[23] Santos, M.J., Khanna, S., Hestir, E.L., et al. 2016. Measuring landscape-scale spread and persistence of an invaded submerged plant community from airborne remote sensing. Ecological Applications. 26(6):1733-1744.
[24] Petrasova, A., Mitasova, H., Petras, V., and Jeziorska, J. (2017). Fusion of high-resolution DEMs for water flow modeling. Open Geospatial Data, Software and Standards. 2. 10.1186/s40965-017-0019-2.
[25] Belliss, S. and Pairman, D. 2009. Detectibility of Small Manchurian Wild Rice Infestations around the Kaipara Harbour, Northland Using High Resolution Satellite Imagery from Quickbird/KiwImage. Landcare Research Contract Report: LC0809/119. http://envirolink.govt.nz/assets/Envirolink/690-nlrc91.pdf.
[26] Martin, S., Nicolas, H., Bottner, B., et al. 2010. Mapping and Monitoring of an Aquatic Invasive Plant (Ludwigia grandiflora) with Multispectral Remote Sensing in a Large Wetland in West of France.Presented at International Symposium on Aquatic Plants - Plants in hydrosystems: from functional ecology to weed research, Poznan, POL (2012-08-27 - 2012-08-31).
[27] Baluja, J., Diago, M.P., Balda, P., Zorer, R. et al. 2012. Assessment of Vineyard Water Status Vriability by Thermal and Multispectral Imagery Using an Unmanned Aerial Vehicle. Irrig. Sci. 30:511-522.
[28] Turner, D., Lucieer, A. and Watson, C. 2012. An Automated Techniquue for Generating Heorectified Mosaics from Ultra-High Resolution Unmanned Aerial Vehicle (UAV) Imagery, Based on Structure from Motion (SfM) Point Clouds. Remote Sensing. 4(5):1392-1410.
[29] Candiago, S., Remondino, F., De Giglio, M., Dubbini, and Gattelli, M. 2015. Evaluating Multispectral Images and Vegetation Indicies for Precision Farming Applications from UAV Images. Remote Sensing. 7:4026-4047.
[30] Hayfield, T. and Racine, J.S. 2008. Nonparametric Econometrics: The np Package. Journal of Statistical Software 27:5. http://www.jstatsoft.org/v27/i05/.
[31] Wickham, H. 2009. ggplot2: Elegant Graphics for Data Analysis. Springer-Verlag New York. https://cran.r-project.org/web/packages/ggplot2/index.html.
[32] R Core Team (2018). R: A language and environment for statistical computing. R Foundation for Statistical Computing, Vienna, Austria. URL https://www.R-project.org/.
[33] Adam, E., Mutanga, O., and Rugege, D. 2010. Multispectral and hyperspectral remote sensing for identification and mapping of wetland vegetation: a review. 18(3):281- 296.
[34] Vega, F.A., Ramirez, F.C., Saiz, M.P., and Rosua, F.O. 2015. Multi-temporal imaging using an unmanned aerial vehicle for monitoring a sunflower crop. Biosystems Engineering. 132:19-27.

Downloaded From: https://www.spiedigitallibrary.org/conference-proceedings-of-spie on 22 Jan 2020
Terms of Use: https://www.spiedigitallibrary.org/terms-of-use

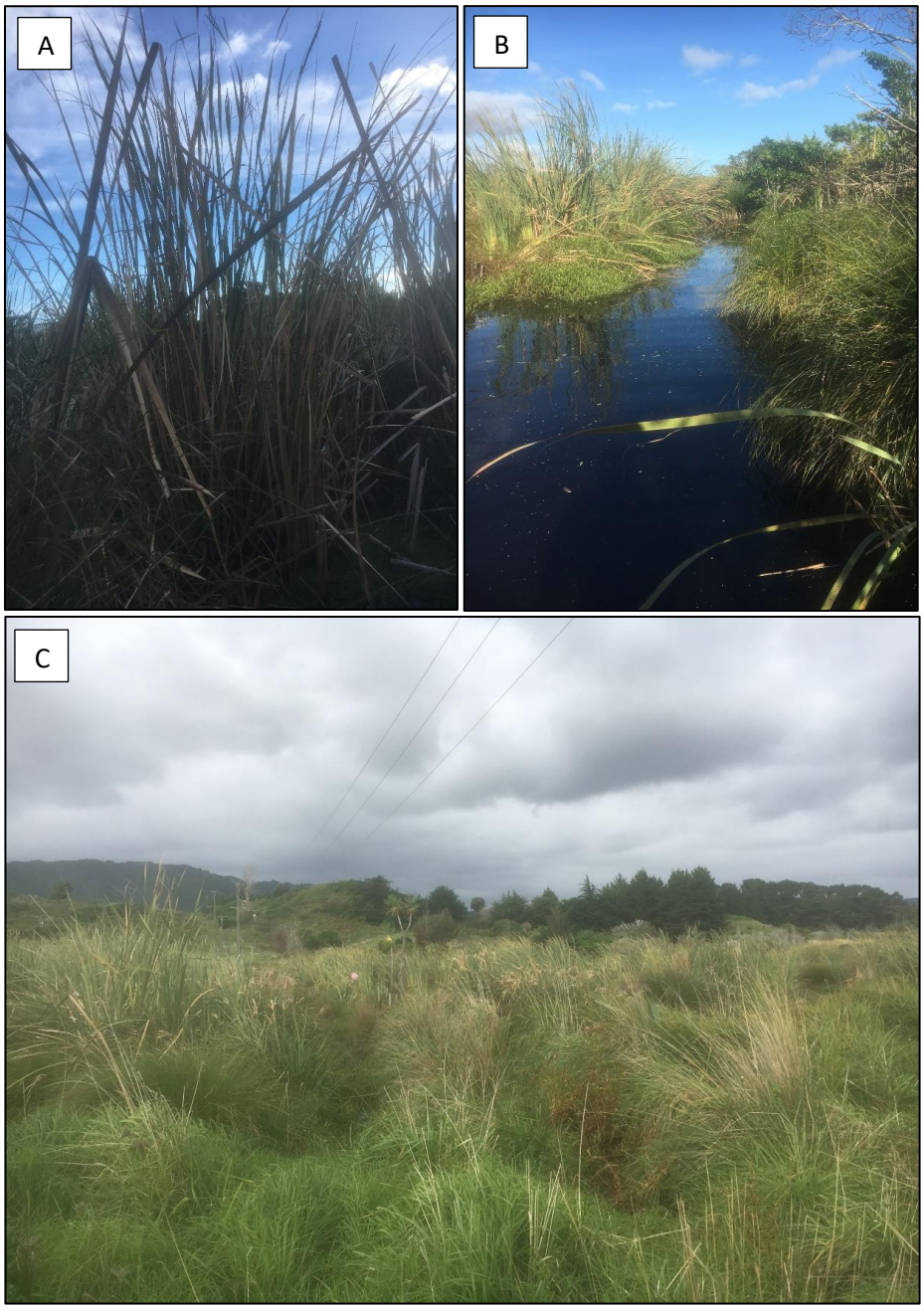

Figure 1. Manchurian Wild Rice growth habit and invaded habitat examples. (A. Typical MWR growth structure with coarse leaves ranging 1-4 m in height/length.; B. Encroachment of drainage canal by invading MWR.; C. Waterlogged pastureland with clumps of MWR spread throughout causing flooding issues). Often, livestock production is reduced due to the invasion of MWR into pastureland and can cause significant drainage issues in water catchment zones.

Downloaded From: https://www.spiedigitallibrary.org/conference-proceedings-of-spie on 22 Jan 2020
Terms of Use: https://www.spiedigitallibrary.org/terms-of-use

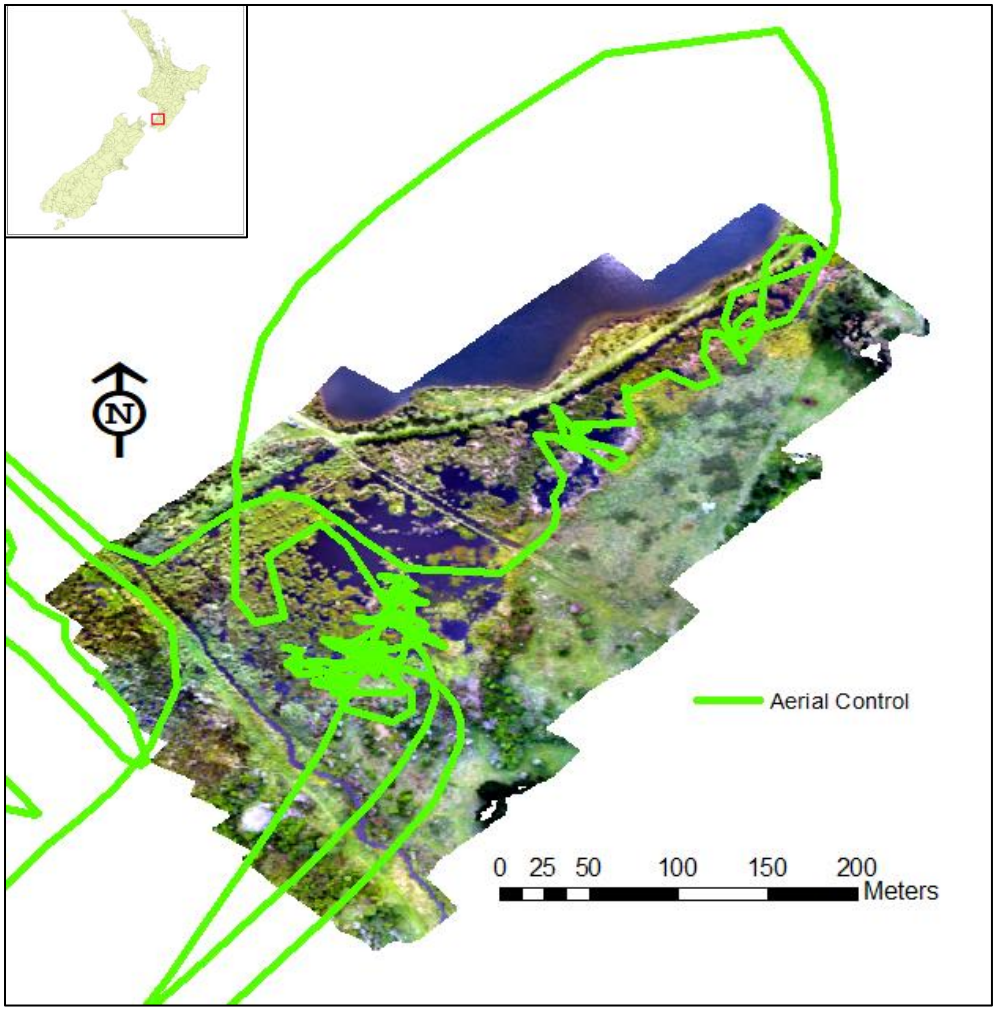

Figure 2. Representation of the study location 1 in Wellington, New Zealand with the first flight plan shown in the provided orthophoto (13.61 ha). The Wellington Region is located at the southernmost portion of New Zealand's North Island. This area is highly biologically productive and is currently impacted by several invasive macrophyte species. However, the area is also supporting populations of nationally threatened aquatic plants, local economies from agricultural operations, and native flora and fauna habitat that is often threatened due to dense stands of exotic vegetation. One of the most ecologically and economically detrimental weed species known to this area is MWR. Aerial control regimes are shown overlain in green on the othrophoto.

Downloaded From: https://www.spiedigitallibrary.org/conference-proceedings-of-spie on 22 Jan 2020
Terms of Use: https://www.spiedigitallibrary.org/terms-of-use

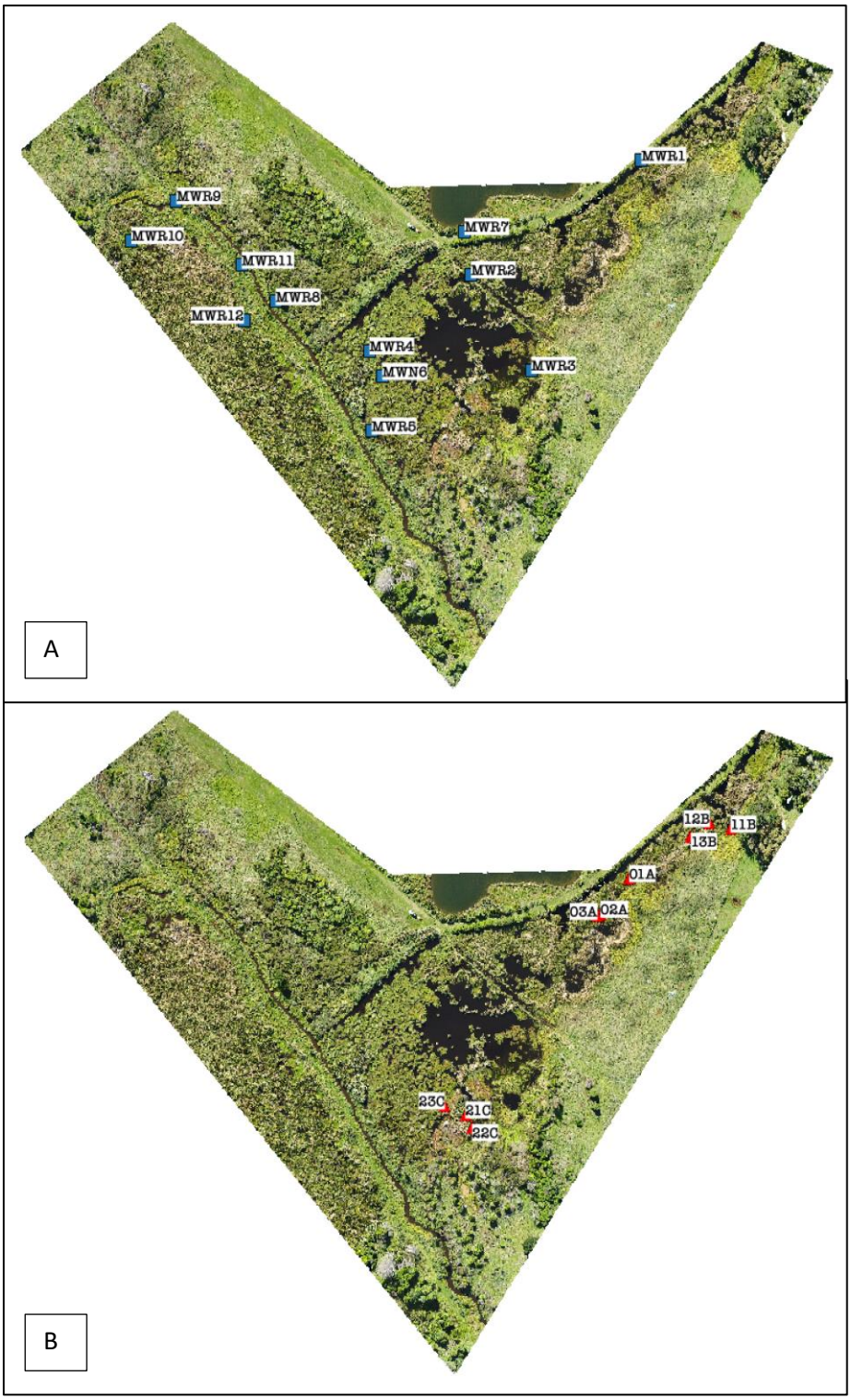

Figure 3. Maps showing an orthomosaic with respective GCP (A) and biomass harvest locations (B). Notably, the accuracy of the handheld GPS used for GCP reference was not ideal for use. However, the GCPs still provide a consistent baseline relative x,y,z-value among all altitudes flown.

Downloaded From: https://www.spiedigitallibrary.org/conference-proceedings-of-spie on 22 Jan 2020
Terms of Use: https://www.spiedigitallibrary.org/terms-of-use

Figure 4. Example of balloon used as a GCP. One of the confines with obtaining accurate and repeatable survey options among aquatic areas is the need for GCPs. Pink party balloons were used to meet the constraints of using GCPs in an aquatic environment. One downside to this method was the time it took to place each balloon, measure the GPS location, and fly the sUAS without the balloon popping. If this area were in need of continued monitoring, then placing a series of permanent poles having visible markings from a nadir perspective would be beneficial. This way, assessment time in the field would only be as long as the flight plan, and permanent GCPs allow for a consistent baseline for temporal comparisons.

Downloaded From: https://www.spiedigitallibrary.org/conference-proceedings-of-spie on 22 Jan 2020
Terms of Use: https://www.spiedigitallibrary.org/terms-of-use

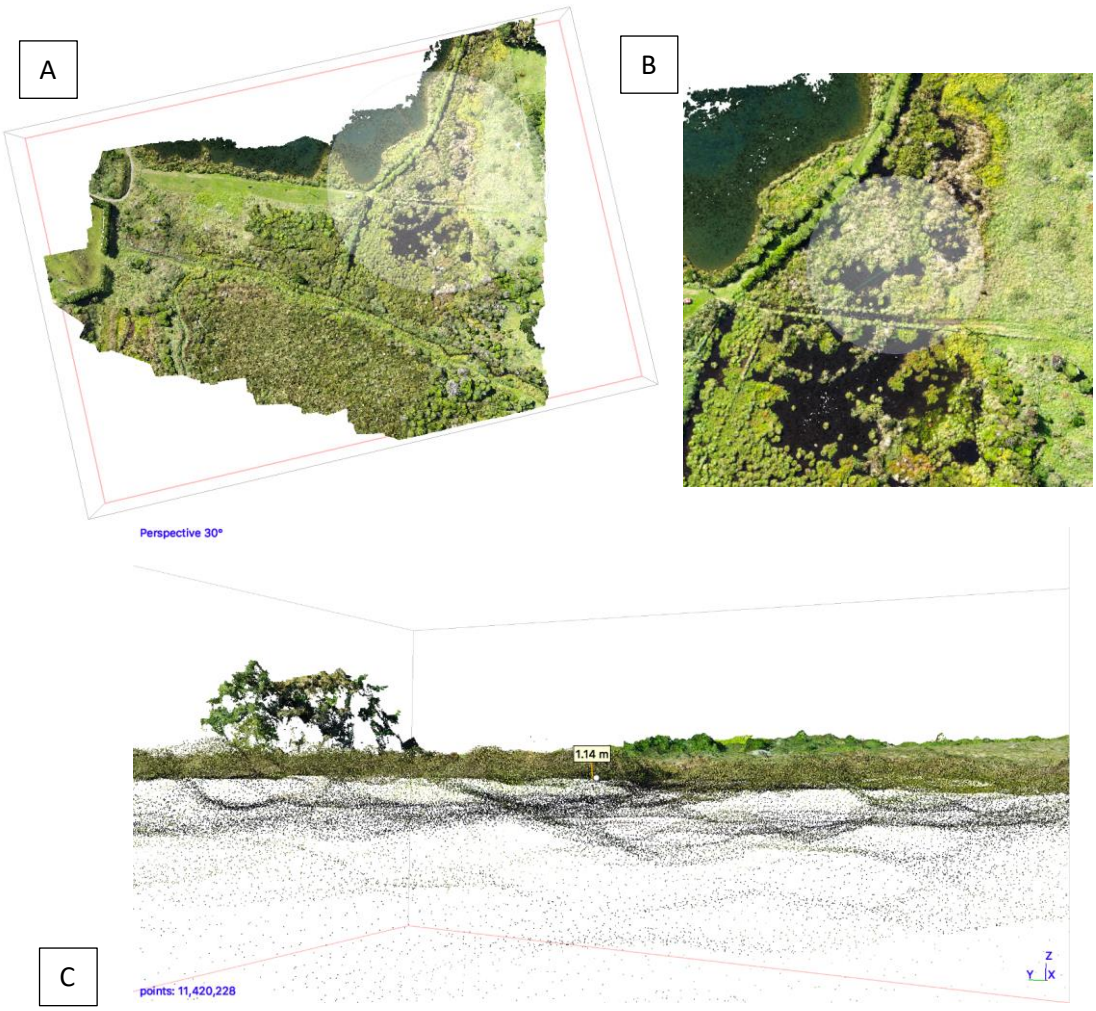

Figure 5. Dense point cloud views in Agisoft PhotoScan of know MWR locations in the map (A. map overview; B. zoomed extent of overview; C. horizontal view of MWR stand with vertical measurement). Height measurements as shown may be validated against DSMs and helicopter treatment path within the map location.

Downloaded From: https://www.spiedigitallibrary.org/conference-proceedings-of-spie on 22 Jan 2020
Terms of Use: https://www.spiedigitallibrary.org/terms-of-use

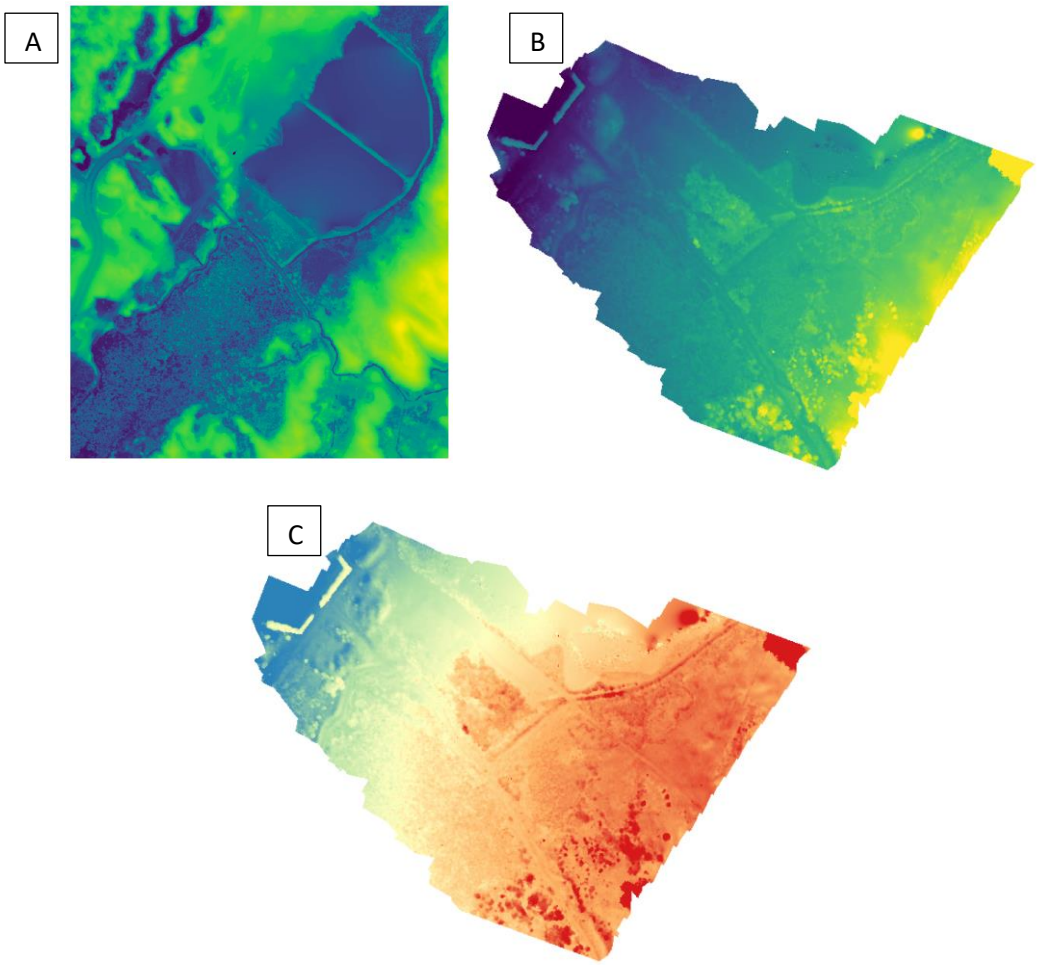

Figure 6. An example of the digital elevation and surface models of the first flight area with an altitude of 120 m. Maps show: A. DEM 1 m Lidar data obtained through Land Information New Zealand (https://www.linz.govt.nz/data/linz-data/elevation-data); B. 12 cm pre-processed DSM done in Agisoft Photoscan; C. Difference model created in GRASS GIS of A and B. Uncorrected elevation data for each map was A: (2.40 – 21.75 m ASL); B: (2.36 – 20.7 m ASL); and C: (0.75 – 14.5 m).

Downloaded From: https://www.spiedigitallibrary.org/conference-proceedings-of-spie on 22 Jan 2020
Terms of Use: https://www.spiedigitallibrary.org/terms-of-use

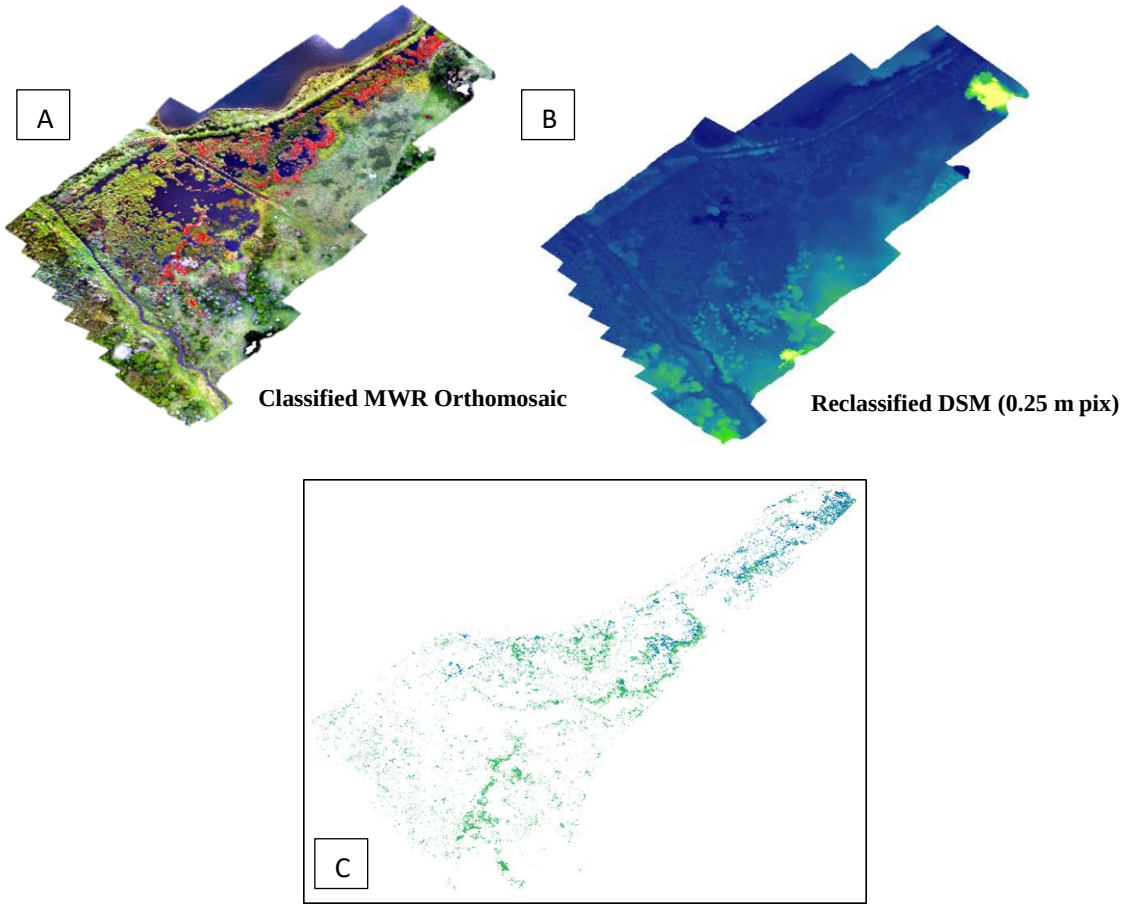

Figure 7. Supervised image classification mapping of MWR from the first study site at 61 m flying altitude. A). Orthophoto generated from this sUAS flight shows MWR classified as red. While the training data needs some manipulation, the classification represents known areas of MWR well. Classification used the biomass collection locations and previous helicopter application logs as an observational test of MWR representation. Supervised classifications of MWR at varying altitudes is being explored. B). The reclassified DSM pixels represent the spatial coverage of each sampling density quadrat. C). Raster image representing MWR plant height values created by extracting the classified MWR orthophoto from the reclassified DSM.

Downloaded From: https://www.spiedigitallibrary.org/conference-proceedings-of-spie on 22 Jan 2020
Terms of Use: https://www.spiedigitallibrary.org/terms-of-use

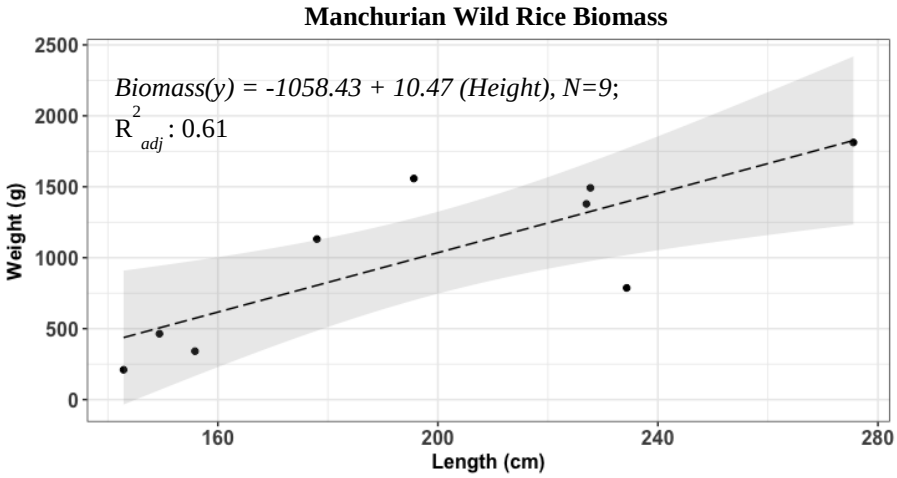

Figure 8. Regression model developed using *in situ* collected biomass and plant height estimates from each density 0.25 m^2 quadrat.

Downloaded From: https://www.spiedigitallibrary.org/conference-proceedings-of-spie on 22 Jan 2020
Terms of Use: https://www.spiedigitallibrary.org/terms-of-use

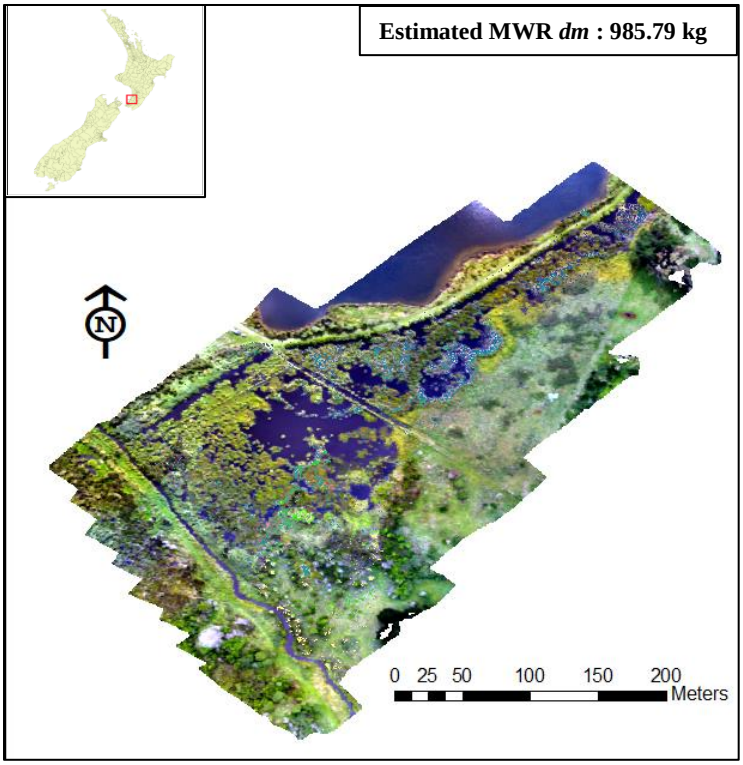

Figure 9. Map deliverable of MWR plant stands represented in location 1 (13.61 ha) estimated at 985.79 kg dry mass from aerially derived plant height estimates and the regression model. Plant stands are shown in the blue-green raster gradient.

Downloaded From: https://www.spiedigitallibrary.org/conference-proceedings-of-spie on 22 Jan 2020
Terms of Use: https://www.spiedigitallibrary.org/terms-of-use

Table 1. GCP balloon locations among both study sites.

GCP Identifier	Latitude	Longitude	Altitude (m)
MWR1	40.850757	175.049869	6.63
MWR2	40.851436	175.048517	6.41
MWR3	40.851974	175.049019	6.79
MWR4	40.851887	175.047712	5.50
MWR5	40.852345	175.047744	7.23
MWN6	40.852031	175.04782	8.43
MWR7	40.851189	175.048456	5.98
MWR8	40.851618	175.046948	4.68
MWR9	40.851054	175.046132	3.49
MWR10	40.851288	175.045775	3.64
MWR11	40.851414	175.046668	2.50
MWR12	40.851728	175.046696	2.69

Downloaded From: https://www.spiedigitallibrary.org/conference-proceedings-of-spie on 22 Jan 2020
Terms of Use: https://www.spiedigitallibrary.org/terms-of-use

Table 2. Destructive biomass harvest of MWR in first study site.

Biomass Identifier	Density Level	Latitude	Longitude
01A	[0-1 m]	40.850935	175.04977
02A		40.851143	175.049544
03A		40.851156	175.049521
11B	[1-2 m]	40.850635	175.05058
12B		40.850606	175.050414
13B		40.850683	175.050261
21C	[>2 m]	40.852317	175.048487
22C		40.852389	175.048543
23C		40.852268	175.048321

Downloaded From: https://www.spiedigitallibrary.org/conference-proceedings-of-spie on 22 Jan 2020
Terms of Use: https://www.spiedigitallibrary.org/terms-of-use